nagra.

Arbeitsbericht NAB 22-03

TBO Rheinau-1-1: Data Report

Dossier VIII Rock Properties and Natural Tracer Profiles

June 2023

J. Iannotta, F. Eichinger, L. Aschwanden & D. Traber

National Cooperative
for the Disposal of
Radioactive Waste

Hardstrasse 73
P.O. Box
5430 Wettingen
Switzerland
Tel. +41 56 437 11 11

nagra.ch

nagra.

Arbeitsbericht NAB 22-03

TBO Rheinau-1-1: Data Report

Dossier VIII Rock Properties and Natural Tracer Profiles

June 2023

J. Iannotta[1], F. Eichinger[1], L. Aschwanden[2] & D. Traber[3]

[1] Hydroisotop GmbH

[2] Rock-Water Interaction, University of Bern

[3] Nagra

Keywords:
RHE1-1, Zürich Nordost, TBO, deep drilling campaign, rock properties, petrophysical parameters, water content, porosity, natural tracer profiles

National Cooperative for the Disposal of Radioactive Waste

Hardstrasse 73
P.O. Box
5430 Wettingen
Switzerland
Tel. +41 56 437 11 11

nagra.ch

Nagra Arbeitsberichte ("Working Reports") present the results of work in progress that have not necessarily been subject to a comprehensive review. They are intended to provide rapid dissemination of current information.

This NAB aims at reporting drilling results at an early stage. Additional borehole-specific data will be published elsewhere.

In the event of inconsistencies between dossiers of this NAB, the dossier addressing the specific topic takes priority. In the event of discrepancies between Nagra reports, the chronologically later report is generally considered to be correct. Data sets and interpretations laid out in this NAB may be revised in subsequent reports. The reasoning leading to these revisions will be detailed there.

December 2023: Replacement of Tab. 1-3 with an updated version.

This Dossier was prepared by Hydroisotop GmbH in close collaboration with the University of Bern. D. Traber was the responsible Nagra project manager.

We are also grateful for the excellent work of the drill-site team who successfully provided sealed core samples according to our specifications.

We thank P. Blaser and M. Unger for editorial work.

Copyright © 2023 by Nagra, Wettingen (Switzerland) / All rights reserved.
All parts of this work are protected by copyright. Any utilisation outwith the remit of the copyright law is unlawful and liable to prosecution. This applies in particular to translations, storage and processing in electronic systems and programs, microfilms, reproductions, etc.

Table of Contents

List of Tables

List of Figures

List of Appendices

App. A: Comprehensive database with results of laboratory analyses (xls format)

App. B: Hydroisotop GmbH lab data report (pdf format)

Note: Appendices are available upon request.

1 Introduction

1.1 Context

To provide input for site selection and the safety case for deep geological repositories for radioactive waste, Nagra has drilled a series of deep boreholes ("Tiefbohrungen", TBO) in Northern Switzerland. The aim of the drilling campaign is to characterise the deep underground of the three remaining siting regions located at the edge of the Northern Alpine Molasse Basin (Fig. 1-1).

In this report, we present the results from the Rheinau-1-1 borehole located in the siting region Zürich Nordost (Fig. 1-2). In the following, the main exploration objectives of this specific borehole are further outlined.

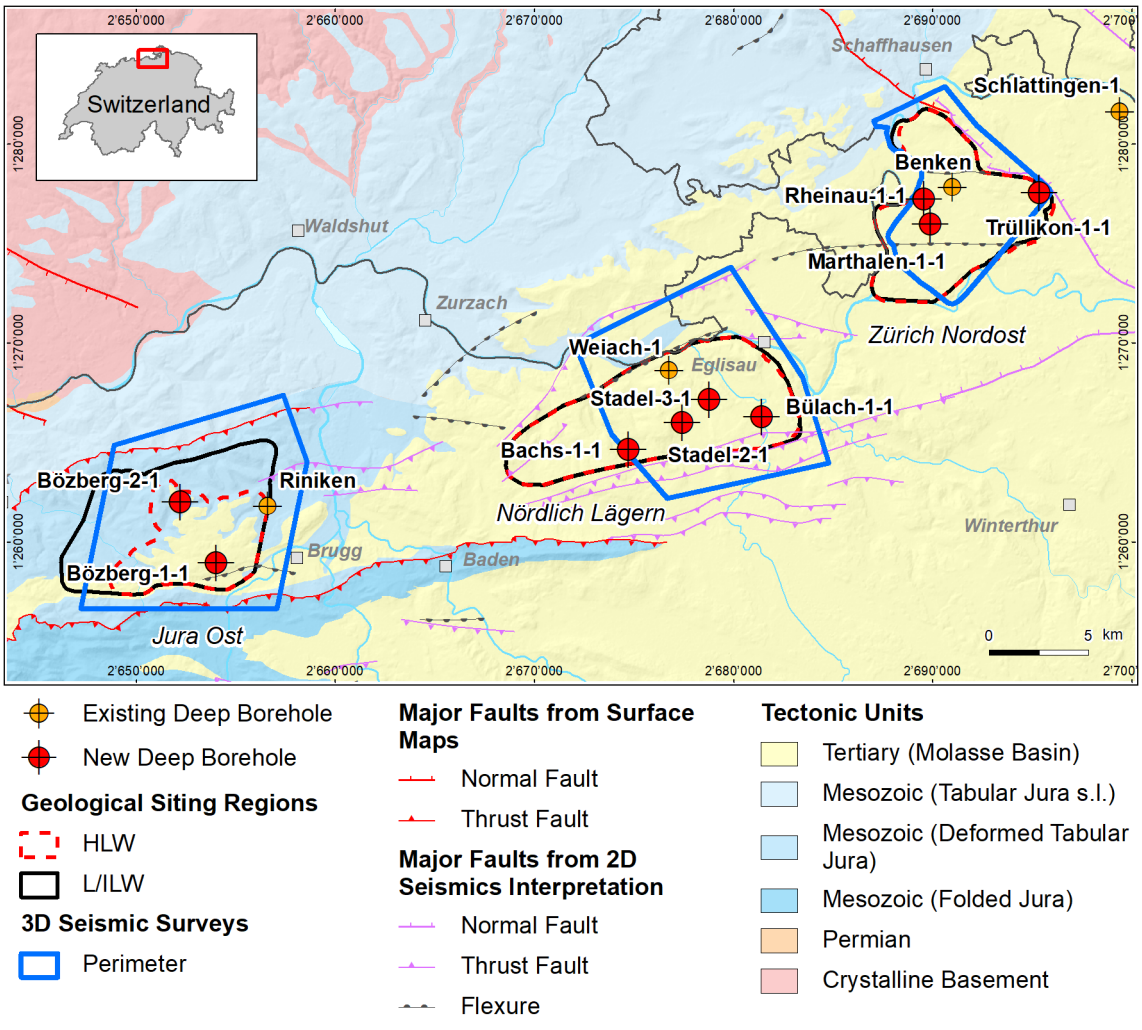

Fig. 1-1: Tectonic overview map with the three siting regions under investigation

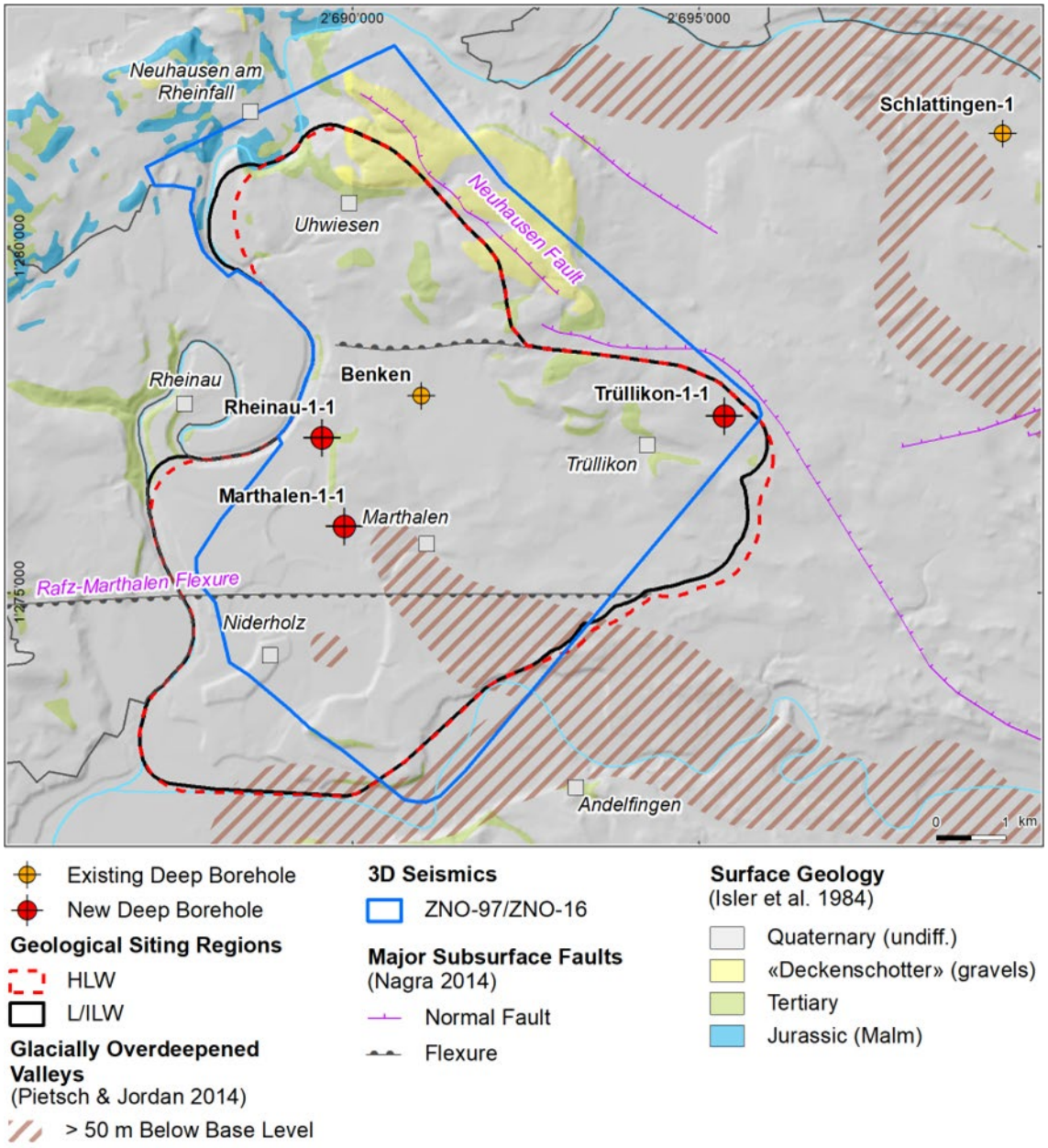

Fig. 1-2: Overview map of the investigation area in the Zürich Nordost siting region with the location of the RHE1-1 borehole in relation to the Benken, TRU1-1 and MAR1-1 boreholes

Exploration objective of the Rheinau-1-1 borehole

In the context of Nagra's TBO project, the Rheinau-1-1 (RHE1-1) borehole is the only deviated borehole. It was planned as a case study with the primary objective of characterising the structural geology of the Opalinus Clay in the area of a steeply dipping fault. Furthermore, dedicated hydrological packer testing and investigations of natural tracers in porewater were conducted to investigate the self-sealing capacity of the Opalinus Clay. More specifically, a stepped constant head injection test was performed in addition to the standard hydraulic packer test to investigate the evolution of transmissivity as a function of effective stress in a fractured interval (*cf.* Dossier VII, Hydraulic Packer Testing for details).

To enable hydraulic testing in the Opalinus Clay with its relatively low strength and high swelling capacity, the maximum borehole deviation (with respect to vertical) was limited to approximately 35° (borehole plunge of 55°). Hence, for the absolute deviation, a trade-off had to be made between maximising the lateral coverage for fracture frequency statistics (large deviation desired) and robust in-situ testing (small deviation desired).

Given the above-outlined scientific goals and related technical requirements, the Rheinau Fault, located immediately east of the Rheinau-1 drill site, was selected for this case study. It is an NNE-SSW trending, steeply dipping fault showing only very minor indications of vertical offsets in seismic amplitude sections. Nevertheless, it was already identified in seismic attribute horizon slices during initial interpretation of Nagra's 3D seismic campaign in the Zürich Nordost siting region (Birkhäuser et al. 2001) and later confirmed during the analysis of follow-up seismic processing products (e.g. Nagra 2019). Fig. 1-3 shows that this fault has a clear seismic attribute expression along the boundaries of the formations below the Opalinus Clay and also along some of the more brittle units above (see horizon slices of the Top Bänkerjoch and Top Villigen Formations shown in Fig. 1-3). However, within the Opalinus Clay, no clear seismic expression is observed. Fig. 1-4 shows the 3D seismic interpretation considered for trajectory planning of the RHE1-1 borehole together with the discussed and executed borehole trajectories.

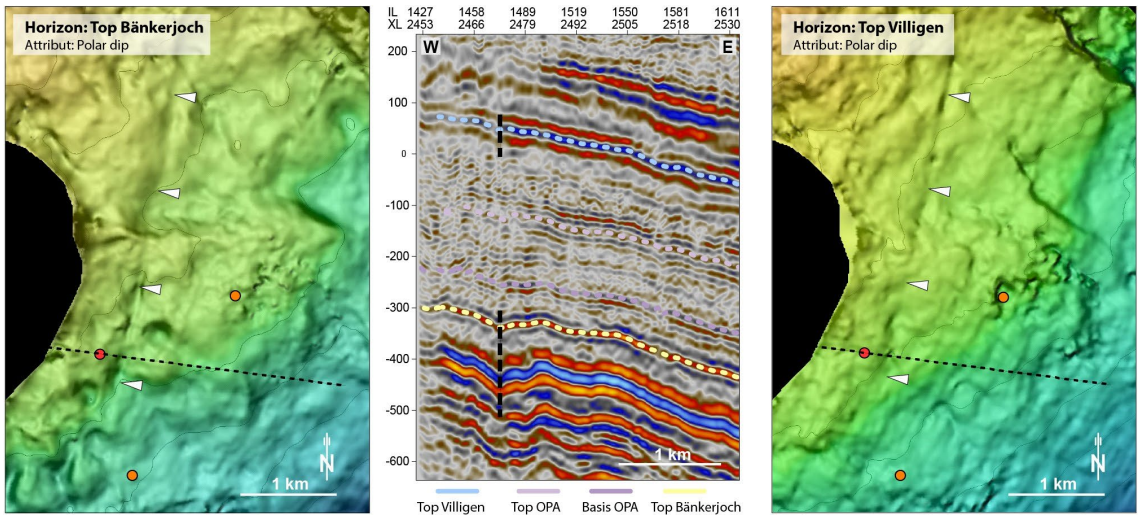

Fig. 1-3: Seismic amplitude cross-section and seismic attribute maps showing the Rheinau Fault

Left and right panels: Seismic attribute maps (polar dip) of a depth-migrated seismic cube (PSDM-A) overlain with depth values (yellowish and blueish colors indicate shallower and larger depths, respectively). The dashed black line indicates the position of the seismic section shown in the central panel. Red and orange dots show the position of the RHE1-1 borehole and neighouring boreholes, respectively. White trianlges mark the lineament representing the Rheinau Fault.

Central panel: Corresponding seismic amplitude section crossing the Rheinau Fault. The vertical axis indicates depth above sea level, and the horizontal axis shows the inline and crossline positions. The approximate trace of the Rheinau Fault above and below the Opalinus Clay is indicated by dashed black lines.

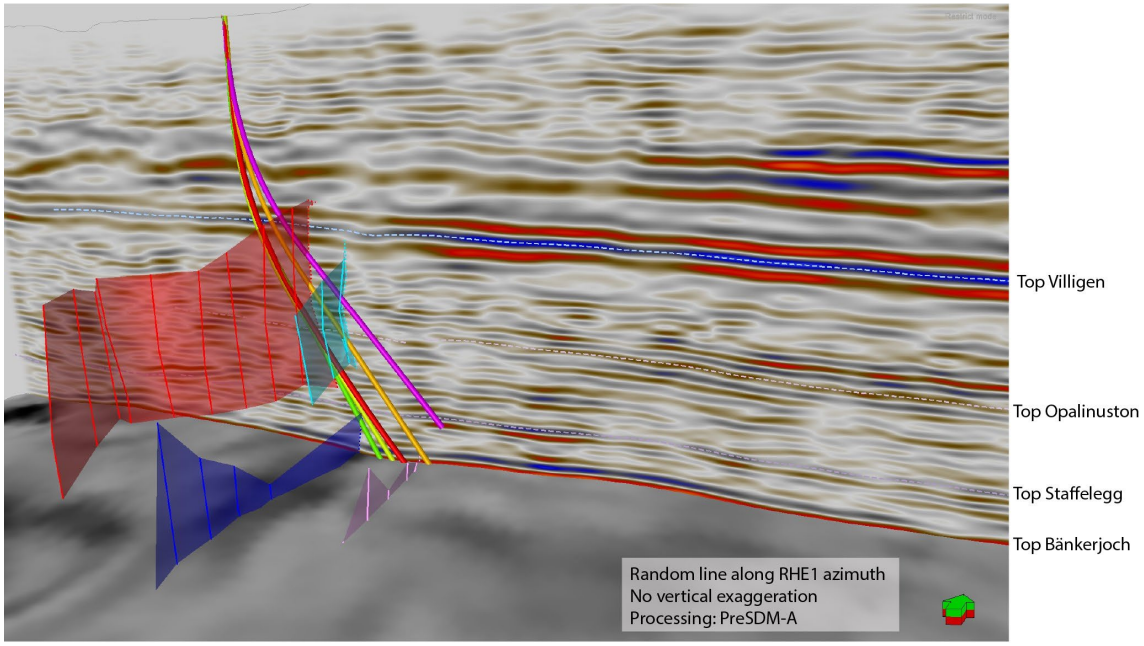

Fig. 1-4: Detailed seismic fault interpretation available for trajectory planning and discussed/ executed well trajectories

Cross-section shows seismic amplitude (seismic processing: pre-stack depth migration PDSM-A). The north direction is indicated by a green-and-red arrow. The vertical distance between the Top Opalinus Clay and Top Staffelegg is ~ 120 m and shows no vertical exaggeration. The horizon slice shows polar dip attribute. Semitransparent subvertical surfaces indicate intepreted faults. The final planned and the drilled trajectories are shown in light green and red, respectively. Other discussed trajectories are shown in yellow, orange and red.

Fig. 1-5 shows a conceptual structural model for the Rheinau Fault incorporating both 3D seismic interpretations and observations from other exploration boreholes as well as from outcrop studies. This conceptual model shows a pronounced mechanical stratigraphy of Northern Switzerland's Mesozoic sedimentary sequence with more focused deformation in the competent units, and distributed deformation in the incompetent units (Roche et al. 2020). Prior to drilling, three hypotheses were formulated on what the RHE1-1 borehole is likely to encounter in the Opalinus Clay. These hypotheses ranged from 1) absence of a distinct fault zone, likely due to a strong degree of strain partitioning within the rheologically weak Opalinus Clay, 2) one or several prominent fault zones, for example revealing cataclastic fault rock or scaly clay as it has been described to occur along larger faults within the Opalinus Clay (Jäggi et al. 2017) and 3) the former but including the occurrence of secondary mineralisations.

As this report represents a data documentation, it deliberately avoids engaging in a synthesis of the observations and test results. Nevertheless, the following results can already be highlighted:

- The drilled trajectory was within close limits compared to the planned well path (see Dossier I for a detailed comparison).
- The borehole did not yield any evidence of a larger-scale fault zone within the Opalinus Clay. However, a number of fault planes have been encountered (*cf.* Dossier V).
- In-situ hydraulic packer tests across these features (*cf.* Dossier VII) yielded hydraulic conductivities similar to undisturbed Opalinus Clay.

- The stepped constant head test demonstrated that a significant enhancement of the flow rate can only be achieved in existing fractures if the fluid pressure is raised considerably and the magnitude of elevated fluid pressure can be maintained (*cf.* Dossier VII).
- Excursions in the profiles of natural tracers can indicate past fluid flow. No such irregularities are seen for the RHE1-1 borehole in the Opalinus Clay (*cf.* Dossier VIII). The stable isotope porewater profiles show characteristics similar to the neighouring vertical boreholes MAR1-1 and Benken.

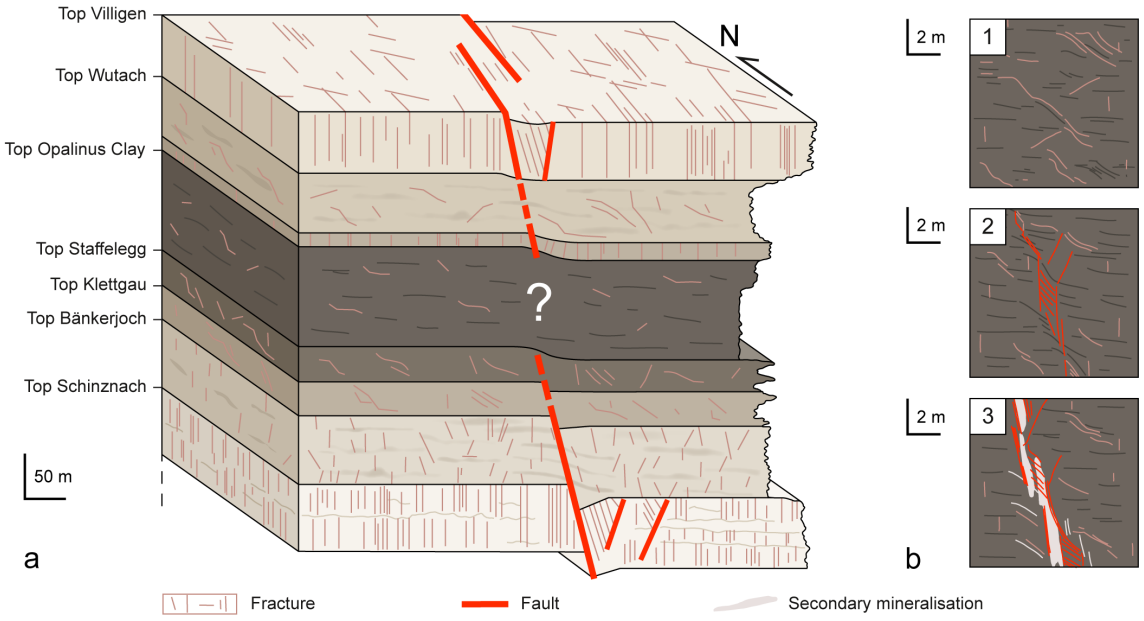

Fig. 1-5: Conceptual structural model of the Rheinau Fault

(a) Conceptual block model. The pronounced mechanical stratigraphy of the Mesozoic sequence in the area is stressed via a schematic weathering profile. The RHE1-1 borehole aimed at characterising the deformation style in the Opalinus Clay constituting a mechanically weak layer in between rheologically stiffer units (e.g. under- and overlying Schinznach/ Bänkerjoch and Villigen/Wutach Formations). According to outcrop records and previous borehole results, these units show a significantly higher frequency of fault planes compared to the Opalinus Clay. In 3D seismics, the Rheinau Fault is also only clearly recognisable at the horizons related to stiffer formations.

(b) Hypothetic deformation characteristics of the Opalinus Clay to be encountered in the RHE1-1 borehole: 1) No exceptional deformation features besides small-scale fault planes as previously observed in vertical boreholes outside of seismically recognised faults. 2) One or several localised zones associated with cataclastic fault rock (e.g. scaly clay) as described for larger fault zones elsewhere (e.g. Jäggi et al. 2017). 3) The above, but also including secondary mineralisation (not to scale on picture).

1.2 Location and specifications of the borehole

The Rheinau-1-1 (RHE1-1) exploratory borehole is the eighth borehole drilled within the framework of the TBO project. The drill site is located in the western part of the Zürich Nordost siting region (Fig. 1-2). The deviated borehole reached a final depth of 827.99 m MD = 745.33 m TVD (true vertical depth)[1]. The borehole specifications are provided in Tab. 1-1.

Tab. 1-1: General information about the RHE1-1 borehole

Siting region	Zürich Nordost
Municipality	Rheinau (Canton Zürich / ZH), Switzerland
Drill site	Rheinau-1 (RHE1)
Borehole	Rheinau-1-1 (RHE1-1)
Coordinates	LV95: 2'689'563.92 / 1'277'235.06
Elevation	Ground level = top of rig cellar: 387.23 m above sea level (asl)
Borehole depth	827.99 m measured depth (MD) = 745.33 m true vertical depth (TVD) below ground level (bgl)
Borehole deviation at total depth (TD)	Inclination from vertical: 38.93° Azimuth from north: 76.25°
Drilling period	19th July – 10th October 2021 (spud date to end of rig release)
Drilling company	PR Marriott Drilling Ltd
Drilling rig	Rig-16 Drillmec HH102
Drilling fluid	Water-based mud with various amounts of different components such as[2]: 0 – 497 m: Polymers 497 – 828 m: Potassium silicate & polymers

The lithostratigraphic profile and the casing scheme are shown in Fig. 1-6. The comparison of the core versus log depth[3] of the main lithostratigraphic boundaries in the RHE1-1 borehole is shown in Tab. 1-2.

[1] Measured depth (MD) refers to the position along the borehole trajectory, starting at ground level, which for this borehole is the top of the rig cellar. For a perfectly vertical borehole, MD below ground level (bgl) and true vertical depth (TVD) are the same. In all Dossiers, depth refers to MD unless stated otherwise.

[2] For detailed information, see Dossier I.

[3] Core depth refers to the depth marked on the drill cores. Log depth results from the depth observed during geophysical wireline logging. Note that the petrophysical logs have not been shifted to core depth, hence log depth differs from core depth.

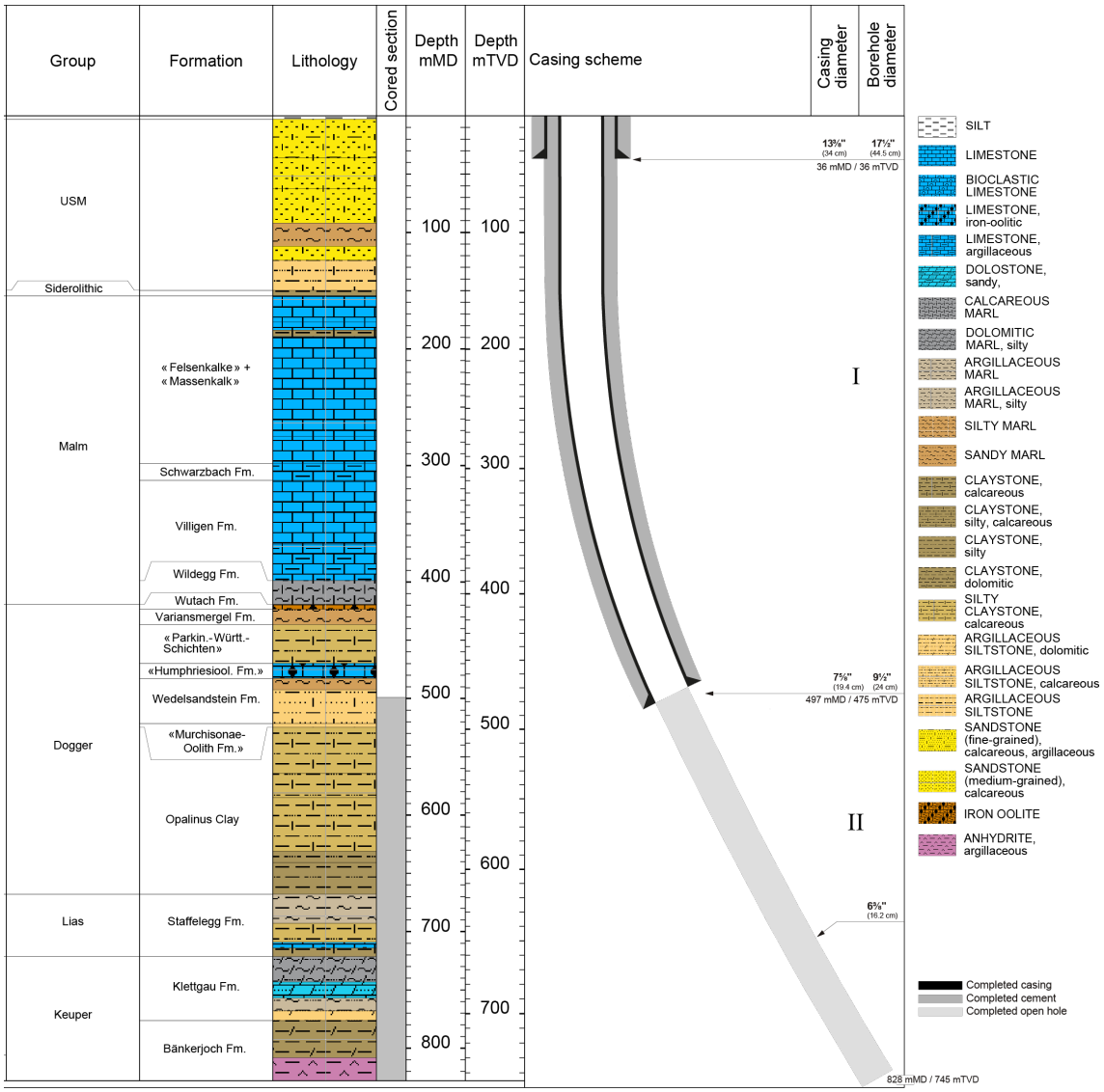

Fig. 1-6: Lithostratigraphic profile and casing scheme for the RHE1-1 borehole[4]

[4] For detailed information, see Dossiers I and III.

Tab. 1-2: Core and log depth for the main lithostratigraphic boundaries in the RHE1-1 borehole[5]

System / Period	Group	Formation		Core top depth in m (MD)			Core top depth in m (TVD)		
Quaternary				**3**		—	**3**		–
Paleogene + Neogene	USM			149.90		—	149.88		–
	Siderolithic			**154.40**		—	**154.37**		–
Jurassic	Malm	«Felsenkalke» + «Massenkalk»		298.10		—	295.71		–
		Schwarzbach Formation		312.70		—	309.70		–
		Villigen Formation		398.80		—	389.75		–
		Wildegg Formation		419.20		—	408.04		–
	Dogger	Wutach Formation		423.40		—	411.78		–
		Variansmergel Formation		436.60		—	423.47		–
		«Parkinsoni-Württembergica-Sch.»		469.80		—	452.23		–
		«Humphriesioolith Formation»		482.80		—	463.20		–
		Wedelsandstein Formation		521.43	521.21	—	495.83	495.64	–
		«Murchisonae-Oolith Formation»		524.61	524.33	—	498.51	498.27	–
		Opalinus Clay		668.07	668.19	—	617.65	617.75	–
	Lias	Staffelegg Formation		**721.46**	**721.50**	—	**660.95**	**660.98**	–
Triassic	Keuper	Klettgau Formation		776.42	776.79	—	704.82	705.11	–
		Bänkerjoch Formation	final depth	827.99	828.24		745.33	745.52	

[5] For details regarding lithostratigraphic boundaries, see Dossiers III and IV; for details about depth shifts (core goniometry), see Dossier V.

1.3 Documentation structure for the RHE1-1 borehole

NAB 22-03 documents the majority of the investigations carried out in the RHE1-1 borehole, including laboratory investigations on core material. The NAB comprises a series of stand-alone dossiers addressing individual topics and a final dossier with a summary composite plot (Tab. 1-3).

This documentation aims at early publication of the data collected in the RHE1-1 borehole. It includes most of the data available approximately one year after completion of the borehole. Some analyses are still ongoing and results will be published in separate reports.

The current borehole report will provide an important basis for the integration of datasets from different boreholes. The integration and interpretation of the results in the wider geological context will be documented later in separate geoscientific reports.

Tab. 1-3: List of dossiers included in NAB 22-03

Black indicates the dossier at hand.

Dossier	Title	Authors
I	TBO Rheinau-1-1: Drilling	M. Ammen & P.-J. Palten
II	TBO Rheinau-1-1: Core Photography	D. Kaehr & M. Gysi
III	TBO Rheinau-1-1: Lithostratigraphy	M. Schwarz, P. Schürch, P. Jordan, H. Naef, R. Felber, T. Ibele & F. Casanova
IV	TBO Rheinau-1-1: Microfacies, Bio- and Chemostratigraphic Analysis	S. Wohlwend, H.R. Bläsi, S. Feist-Burkhardt, B. Hostettler, U. Menkveld-Gfeller, V. Dietze & G. Deplazes
V	TBO Rheinau-1-1: Structural Geology	A. Ebert, S. Cioldi, E. Hägerstedt, L. Gregorczyk & F. Casanova
VI	TBO Rheinau-1-1: Wireline Logging and Micro-hydraulic Fracturing	J. Gonus, E. Bailey, J. Desroches & R. Garrard
VII	TBO Rheinau-1-1: Hydraulic Packer Testing	R. Schwarz, M. Willmann, P. Schulte, H. Fisch, S. Reinhardt, L. Schlickenrieder, M. Voß & A. Pechstein
VIII	TBO Rheinau-1-1: Rock Properties and Natural Tracer Profiles	J. Iannotta, F. Eichinger, L. Aschwanden & D. Traber
IX	*NAB 22-03 does not include a Dossier IX, as no rock-mechanical and geomechanical laboratory tests were conducted.*	
X	TBO Rheinau-1-1: Petrophysical Log Analysis	S. Marnat & J.K. Becker
	TBO Rheinau-1-1: Summary Plot	Nagra

1.4 Scope and objectives of this dossier

The dossier at hand summarises the laboratory work of Hydroisotop GmbH dedicated to rock and porewater characterisation of core materials obtained from the RHE1-1 borehole. The level of ambition is to document observations and measurements and to provide a quality-assured dataset. Compared to other TBO boreholes, only a limited parameter-set was analysed on the cores from borehole RHE1-1. This is in line with the objectives of this borehole (Section 1.1).

Data are evaluated and discussed to some degree, including consistency and plausibility checks. An in-depth discussion, sophisticated modelling efforts and regional comparisons with data from other sites are beyond the scope of this report. An integrated interpretation of all available data will be documented in separate reports.

Throughout this report, rock samples used for analysis are identified by their mid-sample core depth in meter MD.

2 Sampling and applied methods

2.1 Sampling strategy and laboratory programme

In the RHE1-1 borehole, a large number of the sample type PW (porewater) was conditioned onsite as described by Rufer & Stockhecke (2019). For example, in the Opalinus Clay section around one PW sample per drilled meter was conditioned.

Out of the large sample number, a total of 52 samples from RHE1-1 were analysed for this study (from 502 m and 775 m MD). The taken PW samples were sent by Nagra to Hydroisotop GmbH (HI) for the conduction of isotope diffusive exchange experiments for the determination of signatures of porewater stable isotopes. Additionally, the water contents of the core samples were determined gravimetrically and by isotope mass balance (Tab. 2-1). Further hydrochemical, petrophysical and mineralogical/petrographical parameters were not determined.

Investigations were focused on the Opalinus Clay and the adjacent units (Fig. 1-5, Tab. 1-2, Tab. 2-1).

Tab. 2-1: Numbers of samples collected from the different geological units and the corresponding analytical programme

IDE = Isotope Diffusive Exchange Method = Water isotopes; WC = Water Content.

Lithology	**Formation**	**Number of PW samples**	**Analytical programme**	
			IDE	WC
Dogger	Wedelsandstein Fm.	4	×	×
	Opalinus Clay	30	×	×
Lias	Gross Wolf Mb.	1	×	×
	Rietheim Mb.	2	×	×
	Frick Mb.	4	×	×
	Schambelen Mb.	2	×	×
Keuper	Gruhalde Mb.	3	×	×
	Seebi Mb.	2	×	×
	Gruhalde Mb.	1	×	×
	Ergolz Mb.	2	×	×
	Gansingen Mb.	1	×	×

2.2 Analytical methods and methods of raw-data processing

Water contents (gravimetry and isotope mass balance) and isotope data from isotope diffusive exchange experiments conducted by Hydroisotop GmbH were obtained using the same protocol as that applied by the University of Bern, documented in Waber (ed.) (2020). The evaluation of the diffusive exchange experiments was slightly adjusted compared to the documentation in Waber (ed.) (2020). This revised procedure is documented in Chapter 3 of the BUL1-1 report by Mazurek et al. (2021).

3 Results

3.1 Documentation of measured and calculated data

The relevant data were collected in a comprehensive Excel sheet, which also served as calculation base. The full datasets are provided in the electronic Appendix A.

Petrophysical parameters

- Gravimetric water content ($WC_{grav,wet}$) was measured on core pieces after the isotope diffusive exchange experiments and on additional subsamples. See Appendix A for further details.
- The formalisms to calculate water content from isotope diffusive exchange experiments are detailed in Waber (ed.) (2020) and in Mazurek et al. (2021), see also Appendix A.

Porewater stable isotope signatures

- Porewater $\delta^{18}O$ and $\delta^{2}H$ isotope signatures were calculated following the procedure given in Waber (ed.) (2020) and Gimmi & Waber (2020).

Errors

- The error columns refer to analytical uncertainty or instrument precision for measured parameters and to propagated errors for calculated parameters, following the formalisms documented in Waber (ed.) (2020) and Appendix A.

3.2 Petrophysical parameters

Petrophysical parameters are limited to the determination of water contents and water-loss porosity. These investigations were conducted on all 52 samples.

A summary of measured and calculated petrophysical data is given in Tab. 3-1.

Tab. 3-1: Summary of measured and calculated petrophysical data

Regarding (wet) water contents, the table is based on the averages of 3 separate measurements (1 directly measured value on 'extra piece' and from the 2 subsamples used in the diffusive exchange experiments). Water-loss porosity was estimated based on water content and a generic grain density of 2.7 g/cm^3 (see Section 3.2.2). n = number of samples per unit.

							Gravimetry				Isotope mass balance		
Lithology	**Formation/Member**		**Bulk wet density** [g/cm^3]	**Bulk dry density, calculated** [g/cm^3]	**Grain density [g/cm^3]**	**Pycnometer porosity** [–]	**Water content (wet) (105 °C)** [wt.-%]	**Water content (dry) (105 °C)** [wt.-%]	**Water-loss porosity using bulk wet density** [–]	**Water-loss porosity using grain density** [–]	**Water content (wet) based on isotope diff. exch.** [wt.-%]	**Porosity based on isotope diff. exch. using bulk wet density** [–]	**Porosity based on isotope diff. exch. using grain density** [–]
Dogger	Wedelsandstein Fm.	Mean					4.63				4.98		
		Median					4.80				5.05		
		Stdev					0.53				0.51		
		Min					3.59				4.30		
		Max					5.29				5.54		
		n					4				4		
Dogger	Opalinus Clay	Mean					4.88			0.13	5.48		
		Median					4.94			0.13	5.56		
		Stdev					0.61			0.02	0.68		
		Min					3.01			0.08	3.36		
		Max					5.95			0.16	6.61		
		n					30			30	30		
Lias	Staffelegg Fm.	Mean					5.36				6.09		
		Median					5.18				5.76		
		Stdev					0.98				1.41		
		Min					3.30				3.80		
		Max					6.95				8.66		
		n					8				8		
Lias	Klettgau Fm.	Mean					4.65				5.27		
		Median					5.90				6.34		
		Stdev					2.94				3.08		
		Min					0.02				0.05		
		Max					10.35				10.92		
		n					10				10		

3.2.1 Water content

The distribution of water contents in the studied section Dogger – Keuper is shown in Fig. 3-1. The data reflect the average of the two subsamples derived from isotope mass balance (WC_{IsoEx}), the gravimetrically determined water contents on the aliquots used in the isotope diffusive exchange experiments ($WC_{grav, IsoEx}$) and those determined gravimetrically on an additional aliquot dedicated to the water content determination ($WC_{grav, extra\ piece}$). Variability along the different aliquots is generally small (error bars in Fig. 3-1 reflect 1σ deviation among the different aliquots of a sample, i.e., they are also a measure of the lithological heterogeneity of the sample on the cm scale). The comparison of the $WC_{grav, IsoEx}$ with the $WC_{grav, extra\ pieces}$ shows also good agreements (Fig. 3-1). All three measurements are listed in Appendix B.

Water contents from gravimetry and from isotope diffusive exchange correlate well, but the latter are mostly somewhat higher (Figs. 3-1, 3-2). Two samples deviate from the regression lines (Fig. 3-2), which are classified as less reliable according to the quality criteria (*cf.* Section 3.3.1).

Water contents of samples taken between 502 and 667 m depth along borehole from the Dogger units vary generally only slightly along the depth profile with an average of 4.63 ± 0.53 wt.-% for Wedelsandstein Formation samples and 4.88 ± 0.61 wt.-% for Opalinus Clay samples. In the Liassic, the water content first decreases to 3.61 ± 0.31 wt.-% in the Gross Wolf Member and increases again with increasing depth in the Rietheim, Frick and Schambelen Members to 6.92 ± 0.24 wt.-% (Fig. 3-1). In the Keuper, the water contents show a large variation reflecting lithological heterogeneity (Fig. 3-1, Tab. 3-1).

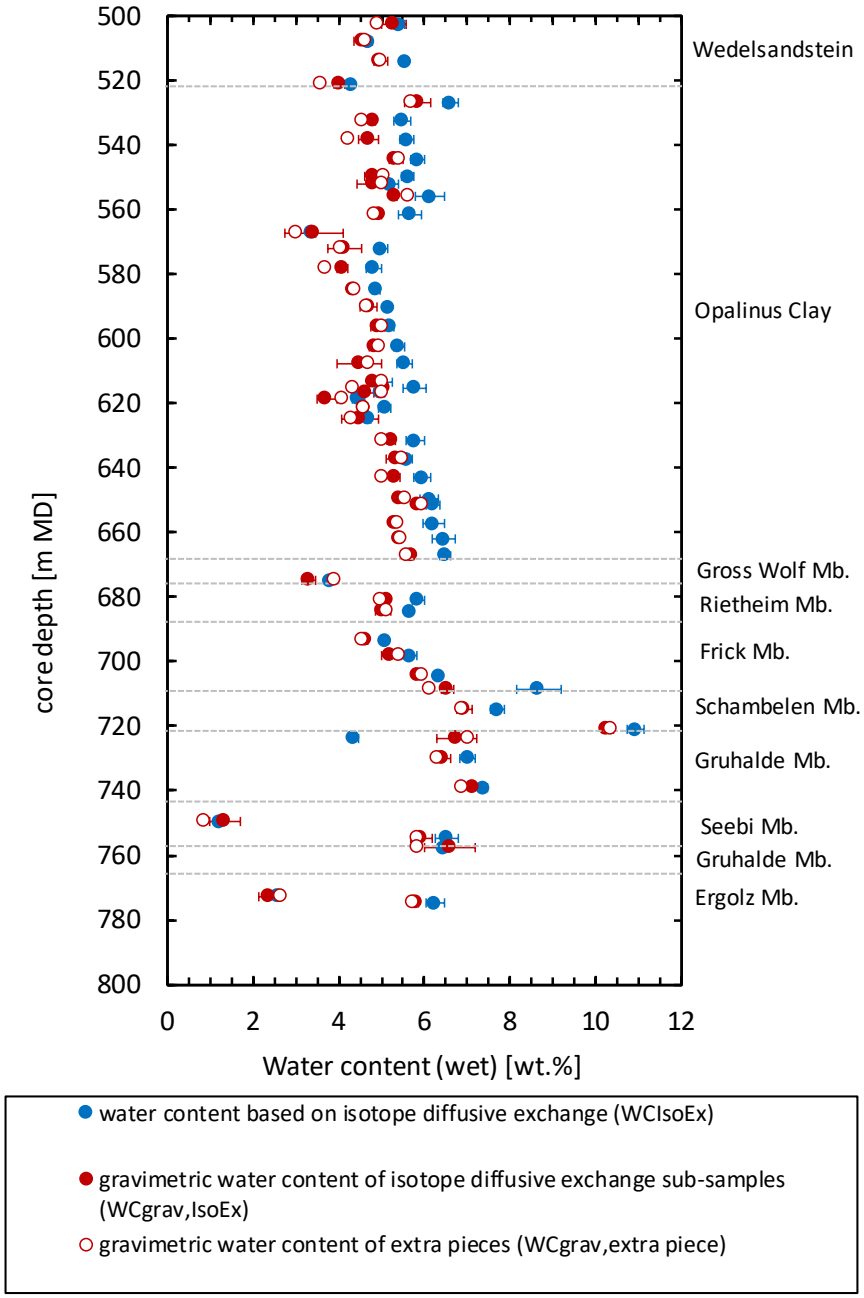

Fig. 3-1: Water content as a function of depth

Error bars for gravimetric water content ($WC_{grav,\ IsoEx}$) indicate 1σ variability among 2 aliquots of the same sample. The gravimetric water content was corrected for any uptake of test water by the rock during the experiments. Error bars for water content from isotope diffusive exchange represent the propagated analytical error. The gravimetric water content of one extra piece for each depth interval was determined additionally.

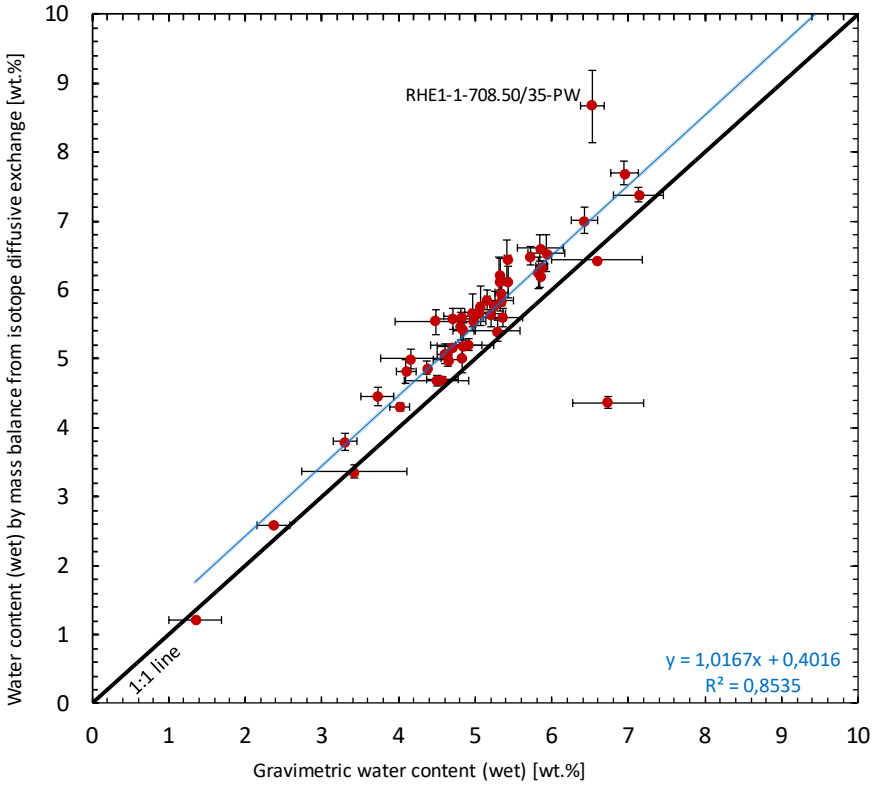

Fig. 3-2: Correlation of water contents based on gravimetry and on isotope diffusive exchange

Note that only the gravimetric water contents obtained from the aliquots used for the isotope diffusive exchange experiments are considered in this graph, so the correlation refers to identical sample materials. Black bars for gravimetric water content indicate 1σ variability among these 2 aliquots. Black bars for water content from isotope diffusive exchange represent the propagated analytical error. Blue regression line excludes the labelled outlier. See Fig. 3-5 for a more detailed comparison.

3.2.2 Porosity

Porosity can be calculated based on water contents obtained by gravimetry (water-loss porosity) or from isotope mass balance and by using either grain or bulk density (Waber ed. 2020). However, no densities were measured on the samples from the RHE1-1 borehole. Assuming fully saturated pore space and a default grain density of Opalinus Clay of 2.7 g/cm^3 (e.g. Zwahlen et al. 2022), one can estimate the water-loss porosity (Tab. 3-1).

The average estimated water-loss porosity of Opalinus Clay amounts to 0.13 ± 0.02 and is shown as profile in Fig. 3-3.

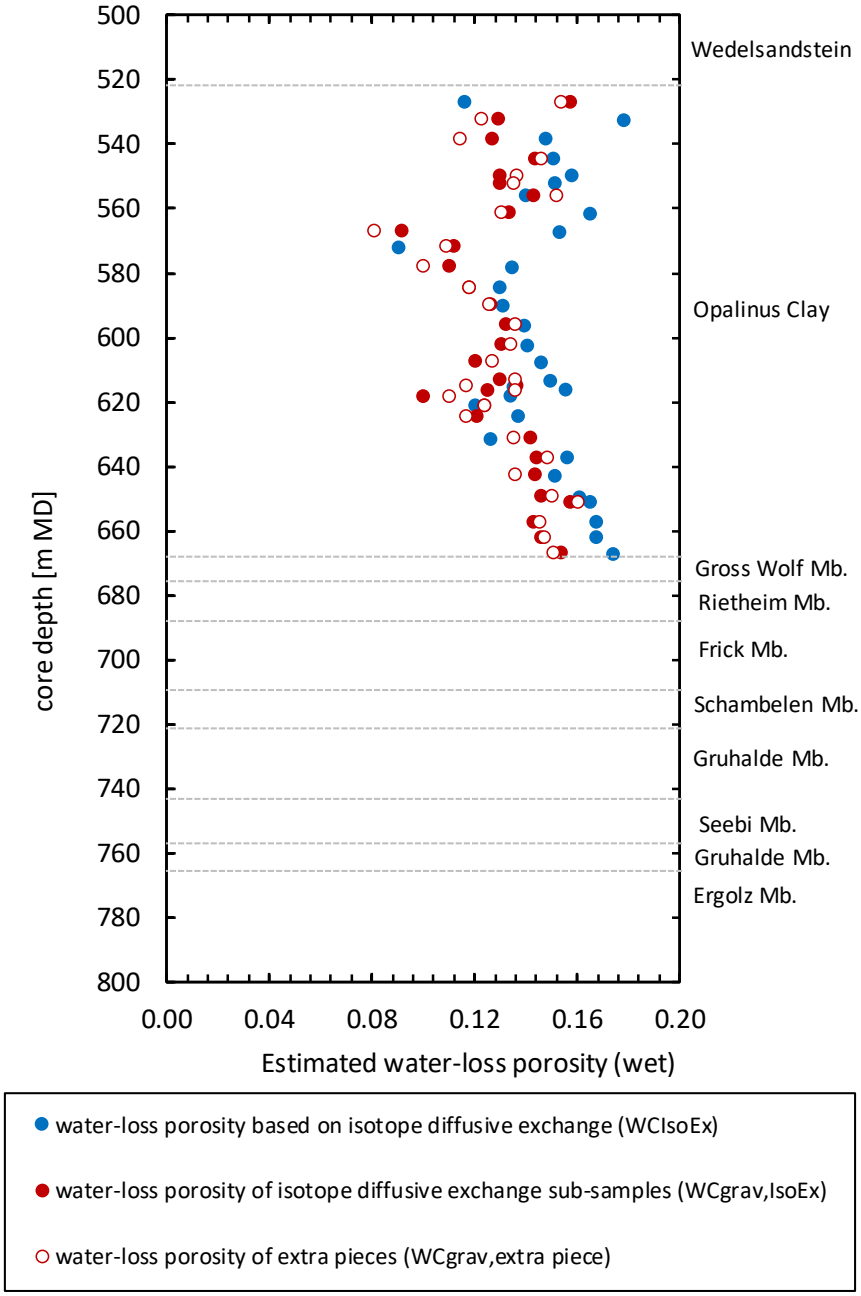

Fig. 3-3: Estimated water-loss porosity as a function of depth

The water-loss porosity is calculated based on a generic grain density of 2.7 g/cm^3.

3.3 Water-isotope data from diffusive exchange experiments

The porewater isotope composition ($\delta^{18}O$, $\delta^{2}H$) was derived by isotope diffusive exchange experiments conducted on core material of 52 samples collected across an interval of 502.8 – 774.8 m depth at the laboratory of Hydroisotop GmbH. The obtained highly resolved profiles for $\delta^{18}O$ and $\delta^{2}H$ cover the lithologies from the Wedelsandstein Formation of the Dogger to the Ergolz Member of the Keuper.

The relevant data produced at Hydroisotop GmbH is summarised in Appendix B.

3.3.1 Data evaluation

3.3.1.1 Experimental and analytical data

The isotope diffusive exchange experiments followed the experimental and analytical protocol given in Waber (ed.) (2020) (see also Appendix B). The evaluation of the experimental and analytical data underlying the derivation of the composition of water stable isotopes in the in situ porewater followed a standardised procedure as detailed below.

In order to qualify for a successful isotope diffusive exchange experiment, the following criteria had to be met (within the propagated analytical uncertainties) by the two experiments (so-called LAB[6] and ICE[7] experiments) conducted for one core sample:

- No severe leakage (evaporation). In most cases, the mass of the experiment container including rock and test water before and after the experiment remained constant (± 0.04 g). If the loss of mass was > 0.04 g, corrections were applied to the measured isotope value of the equilibrated test water by Rayleigh-distillation calculations before calculating the pore-water isotope ratio, assigning the mass loss to evaporation of the initial test water. If the correction of the $\delta^{18}O$ value for evaporation was > 0.5 ‰ VSMOW (typically meaning that the mass loss of test water was > 5% of the initial mass of test water), the porewater isotope value was marked as less reliable.
- Reasonable mass ratio of porewater to test water yielding a change in the isotope signal of the test water after equilibration outside the propagated analytical uncertainty. Porewater to test water ratios as low as 0.1 – 0.2 render the calculated isotope composition of the porewater less reliable, whereas at porewater to test water ratios of < 0.1 it becomes unreliable. The mass of porewater in an experiment is defined by the mass of rock and its gravimetric water content. The latter is not known when starting an experiment.
- Limited mass transfer between rock and test water, i.e. 1) limited transfer of test water to rock (< 0.5 $m_{\text{test water}}$) caused either by high salinity of porewater compared to test water or hydrating mineral phases (e.g. anhydrite, halite) or 2) limited transfer of porewater to test water (< 0.02 g) caused by high salinity of test water compared to porewater. Such mass transfer between rock and test water may lead to isotope fractionation processes whose impacts on the experiments are poorly understood. Porewater isotope data not fulfilling these criteria are kept but classified as less reliable provided that the experiments do not show any further unconformities and that the calculated porewater isotope data and water contents derived from isotope mass balance agree well with those of adjacent samples (i.e. within the propagated analytical uncertainty). If this is not the case (i.e. the data constitute outliers), the experiments are considered as failed.
- Analysis of stable isotopes of test water solutions within the required accuracy.

---

6 LAB: Experiments with laboratory tap water used as test water.

7 ICE: Experiments using test water depleted in ^{18}O and ^{2}H (melt water of Antarctic ice cores).

Almost all of the 52 investigated samples (or 104 individual experiments) passed these criteria, however, for one sample (RHE1-1-766.52/35-PW, Gansingen Member) the experimental data was evaluated as not reliable due to a very low water content and hence a porewater to test water ratio of below 0.1. The calculated porewater isotope composition of this sample will not be shown in the following graphs.

For five samples the experimental data resulted in an elevated uncertainty of the calculated isotope composition of the in situ porewater, i.e., owing to mass transfers between test water and rock sample: The LAB experiment of sample RHE1-1-749.44/35-PW shows a transfer of porewater to test water larger than 0.02 g, whereas four of the individual experiments of samples RHE1-1-698.15/35-PW (LAB), RHE1-1-538.23/35-PW (ICE), RHE1-1-723.80/35-PW (ICE) and RHE1-1-739.12/30-PW (ICE) show a transfer of test water to rock higher than 50% of the initial test water mass. The calculated porewater isotope compositions of these samples were thus classified as less reliable. Such data are marked with open symbols in the following graphs.

3.3.1.2 Calculation of porewater composition and water contents

Porewater $\delta^{18}O$ and $\delta^{2}H$ values were calculated using equation 76 in Appendix A in Waber (ed.) (2020) considering the ratio *q* of the gravimetric water contents of the individual subsamples used in the experiments (for details see Appendix A in Waber ed. 2020). Water contents could then also be calculated by mass balance from the porewater isotope values. The robustness of the calculated porewater $\delta^{18}O$ and $\delta^{2}H$ values was further tested according to the following criteria:

1. A relative difference of less than 20% between the water contents calculated from $\delta^{18}O$ and $\delta^{2}H$ data derived from the experiments with test water depleted in ^{18}O and ^{2}H (ICE subsamples).
2. A relative difference of less than 20% between the average water content calculated by isotope mass balance from $\delta^{18}O$ and $\delta^{2}H$ data and the average of the gravimetric water content of the two subsamples used in the experiments.

If the relative difference in the different water contents is larger than 20%, the calculated porewater $\delta^{18}O$ and $\delta^{2}H$ values are considered less reliable. Such data may still be used for further interpretation by accepting the larger propagated uncertainty; they are marked with open symbols in the following graphs.

All of the 51 samples that passed the experimental quality criteria (*cf.* Section 3.3.1.1; including samples with elevated experimental uncertainties) pass criterion 1 (Fig. 3-4) and only two samples, RHE1-1-708.50/35-PW and RHE1-1-723.80/35-PW, that passed the experimental quality criteria did not pass criterion 2 (Fig. 3-5). The former sample does not show any experimental irregularities and thus, the failure of criterion 2 is likely attributed to lithological heterogeneity of the different subsamples used in the two experiments. For the latter sample test water leaked into the container (ICE experiment), which likely explains the difference between the water contents obtained by gravimetry and isotope mass balance.

All samples that pass the above criterion 2 display a consistent, previously observed relationship between the average water content derived by isotope mass balance and the average of the gravimetric water content of the subsamples used in the experiments whereby almost all samples show an average water content derived by isotope mass balance calculations which is 2 to 17% higher than the gravimetrically determined water contents (Fig. 3-5).

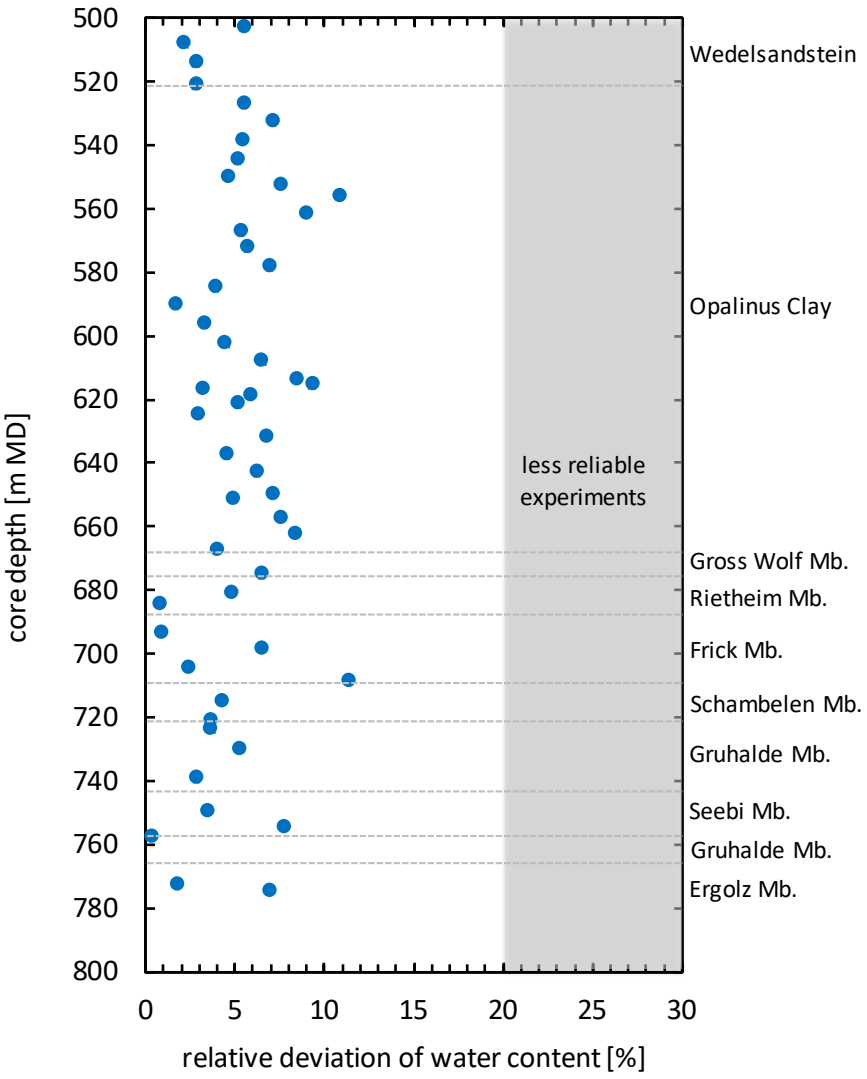

Fig. 3-4: Relative deviation of water contents obtained from $\delta^{18}O$ and $\delta^{2}H$ mass balance

The relative deviation is defined as the difference between the water contents calculated from the equilibrated $\delta^{18}O$ and $\delta^{2}H$ values, respectively, of the experiments with test water depleted in ^{18}O and ^{2}H (ICE) divided by the water content based on $\delta^{2}H$; it is expressed in %. Grey area: Relative deviation of water contents obtained from $\delta^{18}O$ and $\delta^{2}H$ mass balance is > 20%. For samples within this area the calculated porewater $\delta^{18}O$ and $\delta^{2}H$ values would be considered less reliable (not the case for the RHE1-1 dataset).

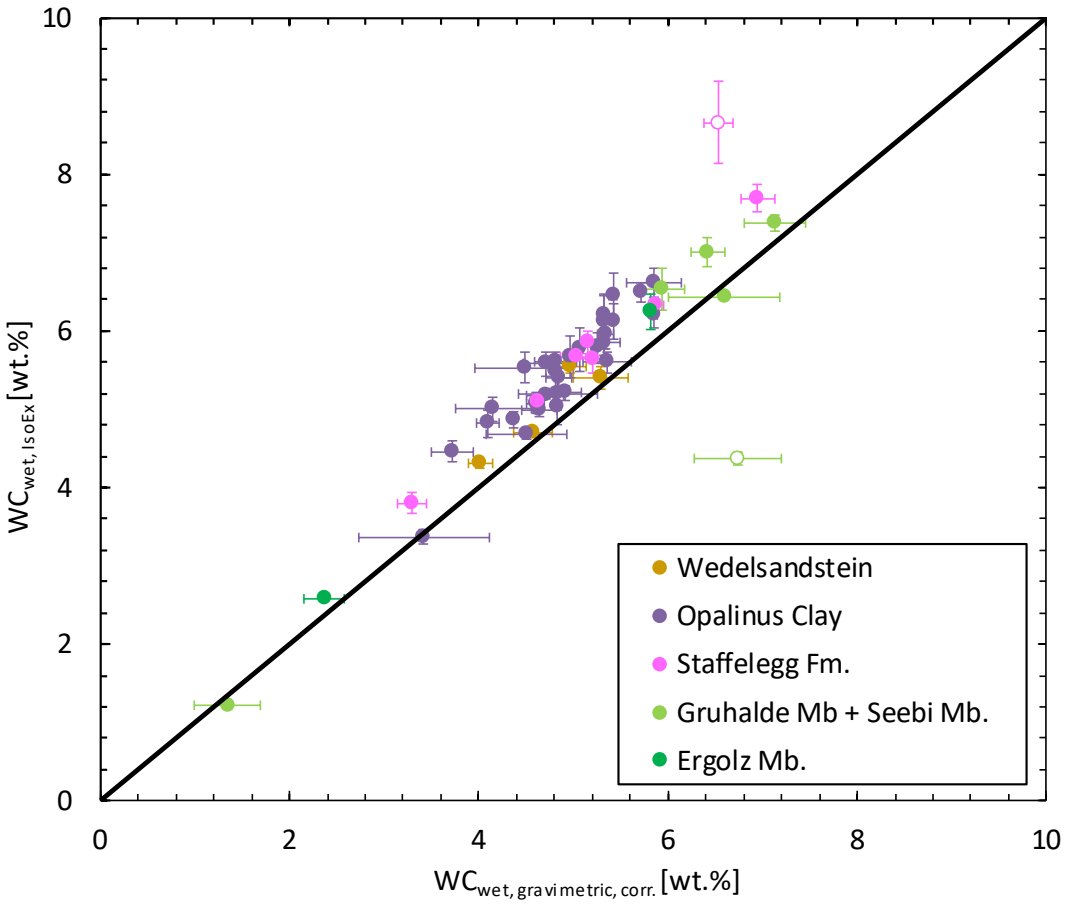

Fig. 3-5: Average water content obtained by water-loss at 105 °C of subsamples LAB and ICE corrected for any uptake of test water by the rock during the experiment ($WC_{wet,\ gravimetric}$) versus average water content calculated from $\delta^{18}O$ and $\delta^{2}H$ mass balance from ICE diffusive exchange experiments ($WC_{wet,\ IsoEx}$)

Open symbols refer to samples showing differences larger than 20% between the average water content derived by isotope mass balance and the average gravimetric water content of the two subsamples used in the experiment. Lias comprises Gross Wolf Mb., Rietheim Mb., Frick Mb. and Schambelen Mb. (*cf.* Tab. 3-1).

3.3.2 $\delta^{18}O$ and $\delta^{2}H$ values of porewater

All the porewater isotope data that pass the various quality criteria are illustrated in Fig. 3-6 as a function of depth. Porewater $\delta^{18}O$ and $\delta^{2}H$ values associated with somewhat larger uncertainties are shown but marked with open symbols in the following graphs.

3.3.2.1 Depth profiles of porewater isotope composition

The porewater $\delta^{2}H$ values remain almost constant across the Wedelsandstein Formation and Opalinus Clay though they slightly decrease from around 596 m towards the top of the Gross Wolf Member (Lias). Across the Lias (Gross Wolf Member, Rietheim Member, Frick Member and Schambelen Member) and the Gruhalde Member (Keuper) they further decrease and reach a

minimum δ^2H value of -61.6 ‰ VSMOW at around 750 m depth in the Seebi Member (value classified as less reliable). Across the remainder of the Keuper (Gruhalde and Ergolz Members) the δ^2H values become more enriched again up to -53.8 ‰ VSMOW at around 775 m depth.

The $\delta^{18}O$ values of the porewater show a similar trend though $\delta^{18}O$ values clearly start to decrease from the Wedelsandstein Formation ($\delta^{18}O$ value of -5.29 to -5.21 ‰ VSMOW) across half of the Opalinus Clay. From around 602 m depth the decrease in $\delta^{18}O$ values becomes steeper towards a minimum of -9.42 ‰ VSMOW at the same depth of around 750 m as observed for δ^2H. From there the trend reverses and $\delta^{18}O$ signatures start to increase, reaching values of -8.30 ‰ VSMOW at around 775 m depth (Ergolz Member).

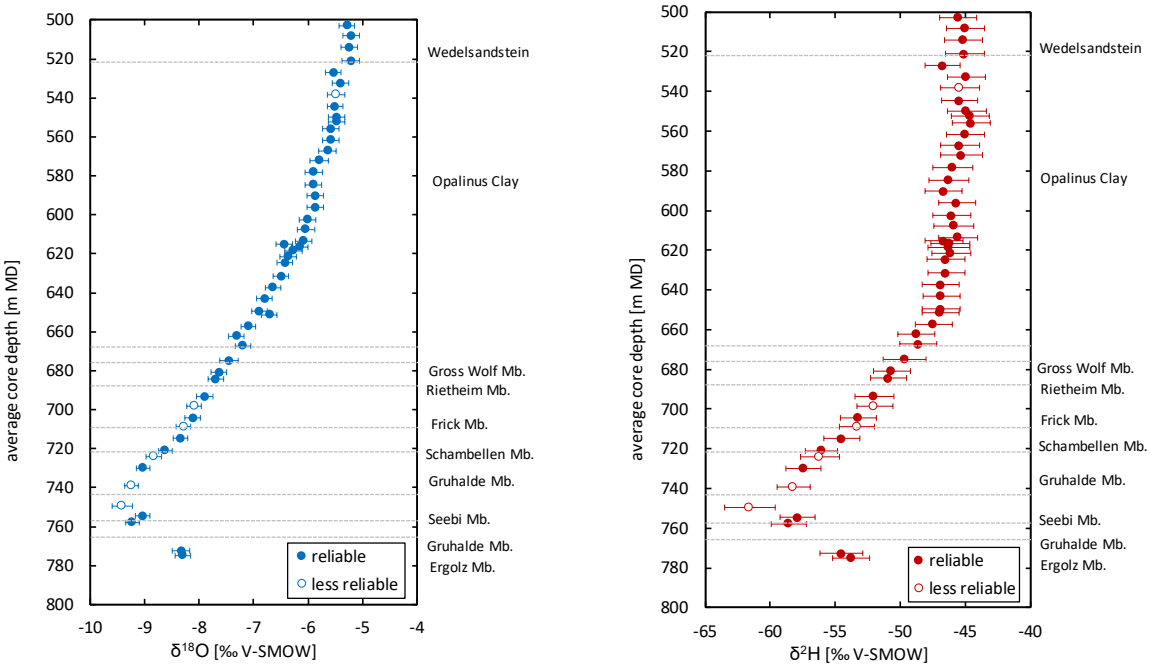

Fig. 3-6: Depth distribution of porewater $\delta^{18}O$ and δ^2H values obtained from isotope diffusive exchange experiments

Open symbols refer to porewater isotope values which are less reliable owing to experimental artefacts (see text).

The slightly different shapes of the $\delta^{18}O$ and δ^2H profiles are also illustrated in Fig. 3-7, which shows the depth profile of deuterium excess (defined as $\delta^2H - 8 \times \delta^{18}O$; deuterium excess is +10 ‰ for a sample that lies on the Global Meteoric Water Line (GMWL), lower values of deuterium excess reflect sample positions to the right of the GMWL in a plot of δ^2H versus $\delta^{18}O$; note that the deuterium excess as used at this stage carries no direct implications about the palaeoclimate at the time of infiltration; it is the result of several interactions – some acting in the deep underground).

The shape of the deuterium excess profile is smooth with only minimal scatter (Fig. 3-7). From the Wedelsandstein Formation the deuterium excess increases towards the base of the Opalinus Clay to a value of around 9.8 ‰. Hence, considering the calculated errors the porewater isotope

value of the sample from the base of the Opalinus Clay lies on the GMWL. The deuterium excess further increases continuously across the Lias towards a maximum of 15 ‰ at around 739 m depth (Seebi Member). From there the deuterium excess scatters slightly. Towards the Ergolz Member at 773 and 775 m depth, the deuterium excess decreases again slightly to 12.1 and 12.7 ‰.

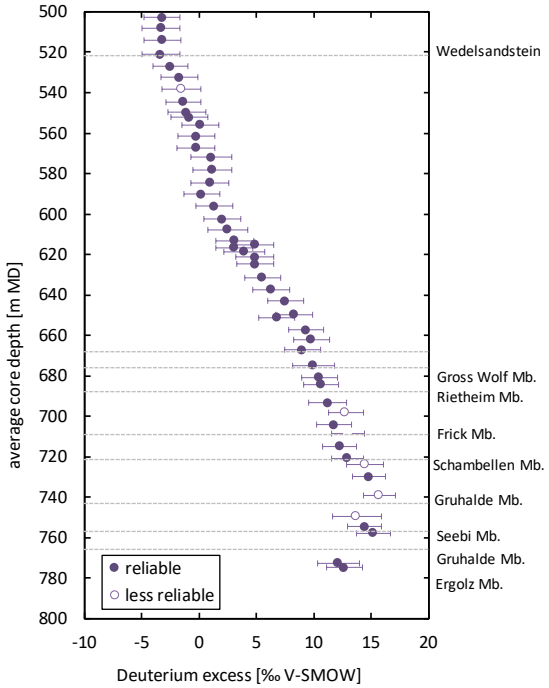

Fig. 3-7: Depth trend of deuterium excess in porewater based on the isotope diffusive exchange technique

Deuterium excess is +10 ‰ for a sample that lies on the GMWL. Lower values of deuterium excess reflect sample positions to the right of the GMWL in a plot of δ^2H versus $\delta^{18}O$. Note that the deuterium excess as used at this stage carries no genetic implications about the origin of H_2O, e.g. on palaeoclimate at the time of infiltration. Open symbols refer to samples which are less reliable owing to experimental artefacts (see text).

3.3.2.2 $\delta^{18}O$ versus δ^2H and comparison with Global Meteoric Water Line

In the $\delta^{18}O$ – δ^2H diagram (Fig. 3-8) some remarkably regular and linear trends can be observed.

Porewater isotope signatures of the Wedelsandstein Formation and Opalinus Clay samples are located to the right of the GMWL whereby the sample from the base of the Opalinus Clay lies on the GMWL. From the top of the Lias and with increasing depth, the porewater isotope signatures shift to the left of the GMWL and towards more depleted $\delta^{18}O$ and δ^2H values though the samples from the Ergolz Member increase again towards less negative $\delta^{18}O$ and δ^2H values.

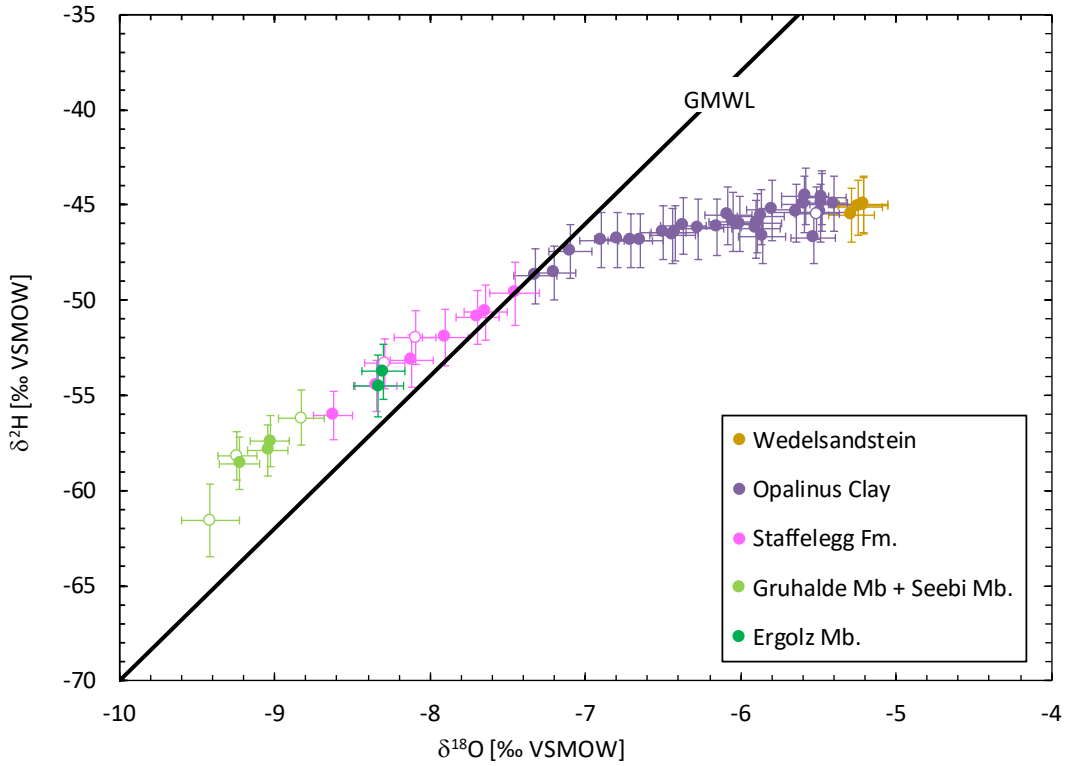

Fig. 3-8: δ^2H versus $\delta^{18}O$ values of porewater obtained from isotope diffusive exchange experiments

GMWL = Global Meteoric Water Line ($\delta^2H = 8 \times \delta^{18}O + 10$ ‰ VSMOW), open symbols refer to porewater isotope values which are less reliable owing to experimental artefacts (see text).

4 Final remarks and main conclusions

This report presents the spatially highly resolved dataset of the composition of stable isotopes of porewater in the inclined section of the RHE1-1 borehole. The depth profiles across the Opalinus Clay and the adjacent units show similar shapes as observed for other boreholes in the ZNO area. In the $\delta^{2}H$ – $\delta^{18}O$ diagram, a similar continuous evolution from values to the right of the GMWL (Wedelsandstein Formation, upper Opalinus Clay) towards meteoric signatures in the lower part of the profile is evident. Porewater isotope compositions in the Klettgau Formation plot somewhat to the left of the GMWL. This characteristic signature was also observed in groundwater samples from the Keuper aquifer in the nearby boreholes of Benken (Waber & Traber 2022) and Trüllikon-1-1 (Aschwanden et al. 2021). The profiles of the stable isotopes show no excursions related to the tectonic setting of this borehole (see Chapter 1).

5 References

Aschwanden, L., Camesi, L., Gimmi, T., Jenni, A., Kiczka, M., Mäder, U., Mazurek, M., Rufer, D., Waber, H.N., Wersin, P., Zwahlen, C. & Traber, D. (2021): TBO Trüllikon-1-1: Data Report. Dossier VIII: Rock properties, porewater characterisation and natural tracer profiles. Nagra Arbeitsbericht NAB 20-09.

Birkhäuser, P., Roth, P., Meier, B. & Naef, H. (2001): 3D-Seismik: Räumliche Erkundung des mesozoischen Sedimentschichten im Zürcher Weinland. Nagra Technischer Bericht NTB 00-03.

Gimmi, T. & Waber, H.N. (2020): Isotope diffusive exchange method: Novel calculations of porewater stable isotopes and water contents, considering mass differences of rock and water and evaporation. Personal communication of electronic calculation file.

Isler, A., Pasquier, F. & Huber, M. (1984): Geologische Karte der zentralen Nordschweiz 1:100'000. Herausgegeben von der Nagra und der Schweiz. Geol. Komm.

Jäggi, D., Laurich, B., Nussbaum, C., Schuster, K. & Connolly, P. (2017): Tectonic structure of the "Main Fault" in the Opalinus Clay, Mont Terri rock laboratory (Switzerland). Swiss Journal of Geosciences 110, 67-84.

Mazurek, M., Aschwanden, L., Camesi, L., Gimmi, T., Jenni, A., Kiczka, M., Mäder, U., Rufer, D., Waber, H.N., Wanner, P., Wersin, P. & Traber, D. (2021): TBO Bülach-1-1: Data Report. Dossier VIII: Rock properties, porewater characterisation and natural tracer profiles. Nagra Arbeitsbericht NAB 20-08.

Nagra (2008): Vorschlag geologischer Standortgebiete für das SMA- und das HAA-Lager. Geologische Grundlagen. Nagra Technischer Bericht NTB 08-04.

Nagra (2014): SGT Etappe 2: Vorschlag weiter zu untersuchender geologischer Standortgebiete mit zugehörigen Standortarealen für die Oberflächenanlage. Geologische Grundlagen. Dossier II: Sedimentologische und tektonische Verhältnisse. Nagra Technischer Bericht NTB 14-02.

Nagra (2019): Preliminary horizon and structure mapping of the Nagra 3D seismics ZNO-97/16 (Zürich Nordost) in time domain. Nagra Arbeitsbericht NAB 18-36.

Pietsch, J. & Jordan, P. (2014): Digitales Höhenmodell Basis Quartär der Nordschweiz – Version 2013 (SGT E2) und ausgewählte Auswertungen. Nagra Arbeitsbericht NAB 14-02.

Roche, V., Childs, C., Madritsch, H. & Camanni, G. (2020): Controls of sedimentary layering and structural inheritance on fault zone structure in three dimensions. A case study from the northern Molasse basin, Switzerland. Journal of the Geological Society 177/3, 493-508.

Rufer, D. & Stockhecke, M. (2019): Field Manual: Drillcore sampling for analytical purposes. Nagra Arbeitsbericht NAB 19-13.

Waber, H.N. (ed.) (2020): SGT-E3 deep drilling campaign (TBO): Experiment procedures and analytical methods at RWI, University of Bern (Version 1.0, April 2020). Nagra Arbeitsbericht NAB 20-13.

Waber, H.N. & Traber, D. (2022): Die Tiefengrundwässer in der Norschweiz und im angrenzenden Süddeutschland: Beschaffenheit, Herkunft und unterirdische Verweilzeit. Mit Beiträgen von M. Heidinger und G. Lorenz. Nagra Technischer Bericht NTB 19-02.

Zwahlen, C., Aschwanden, L., Gaucher, E., Gimmi, T., Jenni, A., Kiczka, M., Müder, U., Mazurek, M., Ross, D., Rufer, D., Waber, H.N., Wersin, P. & Traber, D. (2022): TBO Stadel-2-1: Data Report. Dossier VIII: Rock properties, porewater characterisation and natural tracer profiles. Nagra Arbeitsbericht NAB 22-02.